Atom-resolved surface chemistry studied by scanning tunneling microscopy and spectroscopy

Ph. Avouris and R. Wolkow
IBM Research Division, Thomas J. Watson Research Center, P.O. Box 218, Yorktown Heights, New York 10598
(Received 18 July 1988)

We have used scanning tunneling microscopy and spectroscopy to study the reaction of Si(111)-(7×7) with NH_3. We have found that by use of topographs obtained at different energies, as well as atom-resolved spectra, reacted and unreacted surface sites can be imaged selectively. Thus we have been able to probe the spatial distribution of the surface reaction on an atom-by-atom basis. We find that there are significant differences in reactivity between the various dangling-bond sites on the Si(111)-(7×7) surface. Specifically, rest-atom sites are more reactive than adatom sites and, moreover, center-adatom sites are more reactive than corner-adatom sites. We ascribe the reduced reactivity at adatom sites to the delocalized nature of their dangling-bond state. We suggest that a bonding interaction between adatoms and the Si atoms directly below them is responsible for this behavior—a suggestion supported by electronic-structure calculations. Thus, while reaction at a rest-atom site can be considered a dangling-bond saturation process, reaction at an adatom site involves the formation of a hypervalent (fivefold-coordinated) adatom. We tentatively ascribe the reactivity differences between center and corner adatoms to differences in the strain they induce upon reaction on the dimer bonds. Atom-resolved spectroscopy allows us to probe interactions and charge transfer between surface sites, and for the first time, we can directly observe how chemisorption affects the substrate electronic structure at neighboring *unreacted* sites.

I. INTRODUCTION

Scanning tunneling microscopy (STM) has been used to image the structure of clean surfaces and has provided valuable insight into the nature of surface reconstructions, particularly for semiconductor surfaces.[1] Recently, it also has been used to study the topography of adsorbed, primarily metallic, layers on semiconductors. The ability of STM to provide atomic-scale information on both geometric and electronic structure can lead to a completely new way of studying surface chemistry. Using STM, one should be able to follow the extent and spatial distribution of a surface reaction on an atom-by-atom basis. By probing simultaneously the electronic structure of the different surface sites one then can relate electronic structure and reactivity. Moreover, in this way one could directly probe the interactions between surface sites. The existence of such interactions is inferred in a variety of experiments, such as in vibrational spectroscopy of adsorbates[2] and in the study of adsorption isotherms,[3] where the adsorbate-substrate interaction is studied as a function of coverage. The macroscopic and indirect nature of such measurements, however, does not allow one to discriminate between effects due to modification of the electronic structure of the substrate by the adsorption process and direct lateral interactions between the adsorbates.

In this paper, we present results of scanning tunneling microscopy (STM) and atom-resolved scanning tunneling spectroscopy (AR-STS) studies of the reaction of ammonia (NH_3) with Si(111)-(7×7). This study indicates that the above goals can be achieved by combined STM and AR-STS studies. In previous work[4] we have shown that the reactivity of Si(100)-(2×1) towards a variety of molecular systems is strongly correlated with the presence of surface dangling-bond states. However, all dangling bonds on the Si(100)-(2×1) surface are located on equivalent sites. A far more chemically interesting case and one which would take full advantage of the unique capability of STM to provide atom-resolved information, would be a study of the reactivity of a surface with several structurally distinct active sites. The Si(111)-(7×7) surface is deal in this respect.[5] The nature of the 7×7 reconstruction itself has been the subject of intense study for about 30 years,[6] and the role of STM (Ref. 7) was quite important in the resolution of this problem. Currently, the model proposed by Takayanagi *et al.* [the so-called dimer–adatom–stacking-fault (DAS) model][8] is generally accepted. The DAS model for the 7×7 unit cell is shown in Fig. 1. There are two triangular subunits each surrounded by nine Si dimers; in addition, there is a stacking fault in the left triangle. On the surface there are six triply coordinated Si atoms (labeled *A* and *B* in Fig. 1), so-called *rest atoms.* The top layer is composed of 12 Si *adatoms* (solid circles), and, finally, at the corners of the unit cell there are vacancies usually referred to as *corner holes.* For reasons that will become apparent later in the paper we separate the adatoms into two groups: the ones located next to a corner hole are termed *corner adatoms,* while the other six are called *center adatoms.* The most important chemical effect of the reconstruction is a severe reduction in the number of surface dangling bonds (DB's). While on the unreconstructed Si(111) surface there are 49 DB's, only 19 survive in the 7×7 unit cell. Of these, 12 are located on the two types of adatoms, six on the rest atoms and one on the atom at the bottom of the corner hole. Thus, there are a variety of chemically active surface sites which would allow us to

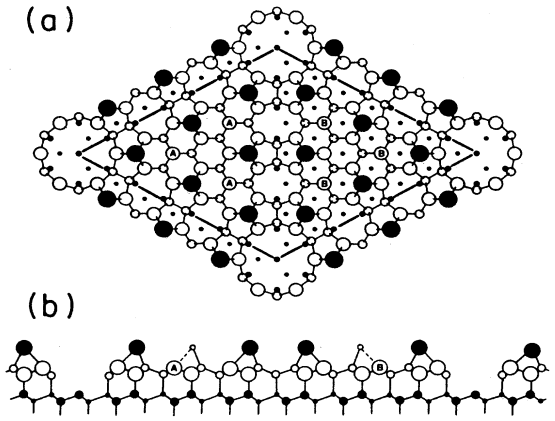

FIG. 1. (a) Top view of the dimer–adatom–stacking-fault (DAS) model of Takayanagi *et al.* (Ref. 8) for the Si(111)-(7×7) surface reconstruction. The 7×7 unit cell is outlined. Atoms at increasing distances from the surface are indicated by circles of decreasing size. The large solid circles denote the 12 adatoms. The circles marked *A* and *B* represent the rest atoms in the faulted and unfaulted halves of the unit cell, respectively. Small open circles denote the dimers, while small solid circles and black dots represent atoms in the unreconstructed layers. (b) Side view. Atoms on the lattice plane along the long diagonal of the surface unit cell are shown with larger circles than those behind them. On the right half of the unit cell the stacking sequence is the same as in bulk Si, i.e., unfaulted; on the left half, the stacking sequence is faulted.

study the role of local structure on reactivity.

The reaction of NH_3 with Si(111)-(7×7) is an interesting one, not only from the basic science point of view, but also because of its use in technology to synthesize silicon nitride—an important electronic material. Early work[9] suggested that NH_3 adsorbs nondissociatively on Si(111)-(7×7); more recent work based on vibrational spectroscopy [electron-energy-loss spectroscopy[10] (EELS)] and photoemission spectroscopy[11,12] has concluded that the adsorption is dissociative, the dissociation products being NH_2 and H bonded to Si.[10,12] In this work we first will discuss topographs of the occupied and unoccupied states of the clean and NH_3-exposed surfaces. We will show that because of the different energy-level structure of the clean and reacted surfaces topographs obtained at different energies allow us to image selectively unreacted atoms and reaction products. Thus, the spatial distribution of the reaction can be directly observed. We then will present and discuss atom-resolved spectra of the clean 7×7 surface, which will allow us to determine the spectral characteristics of the different DB states, as well as possible interactions between these sites present at the clean surface. The corresponding spectroscopy of the partially reacted surface allows us to determine the electronic-structure changes produced by the reaction not only at reacted sites but, for the first time, we can determine the effect of reaction at one site on the electronic structure of a nearby *unreacted* site. From a systematic analysis of topographs and AR-STS maps we determine the relative reactivities of the different surface DB sites. We find significant differences between such sites and discuss these differences in terms of phenomena such as intersite charge transfer, Si hypervalency, and steric strain.

II. EXPERIMENT

The STM experiments were performed in an ion-pumped vacuum chamber having a base pressure of $\sim 1\times10^{-10}$ Torr. The Si crystals used are phosphorus-doped ($\sim 1\Omega$ cm) Si(111) wafers. Sample cleaning involves prolonged heating of the crystal to 700 °C with subsequent removal of the oxide layer by heating to 1030°C for about 1 min. STM types are prepared by electrochemically etching tungsten wires. The tip is mounted on a piezolectric tripod. The sample is placed at the end of a lever which pivots about a point very near the tip. The other end of the lever can be moved by the manual rotation of a fine screw. Backlash in the drive mechanism allows decoupling of the external rotary feed through from the STM. The base of the STM sits on small compression springs on an 8-in. flange. On this base, several plates are stacked, with Viton rubber spacers. The vibrationally isolated top plate holds the piezolectric tripod and lever which carries the sample. The entire vacuum system is mounted on a vibration-isolated table. While recording STM topographs, a feedback circuit controls the tip-surface separation and maintains a constant tunneling current (~ 1 nA). To obtain atom-resolved spectra, topograph measurement is interrupted at every *n*th point (*n* variable), the tip-to-sample separation is temporarily fixed, and the bias voltage is linearly ramped so that an *I-V* curve can be obtained at that point. This synchronized acquisition ensures exact spatial alignment of topographic and spectroscopic information. While this approach leads to large data files, we gain the ability to look at spectroscopic information for every region in a topograph.

III. RESULTS AND DISCUSSION

A. Electronic topography of clean and NH_3-exposed Si(111)-(7×7)

In Fig. 2(a) we show a topograph of the unoccupied states of the clean Si(111) surface obtained with the sample biased at +1.5 V. The 7×7 unit cell is outlined and the 12 adatoms are clearly seen. The two triangular halves of the 7×7 unit appear indistinguishable.[13] In Fig. 2(b) we show a topograph of the occupied states of the 7×7 surface obtained with the sample biased at −1.5 V. The 12 adatoms and the stacking fault are clearly seen. In addition, there is evidence for the presence of rest atoms which give rise to the grey region between adatoms. We find that rest atoms can be clearly imaged at high bias. This is shown in Fig. 2(c) which is a three-dimensional representation of a topograph of the 7×7 unit cell obtained at −3 V.

We can now explore the topography of the reacted Si

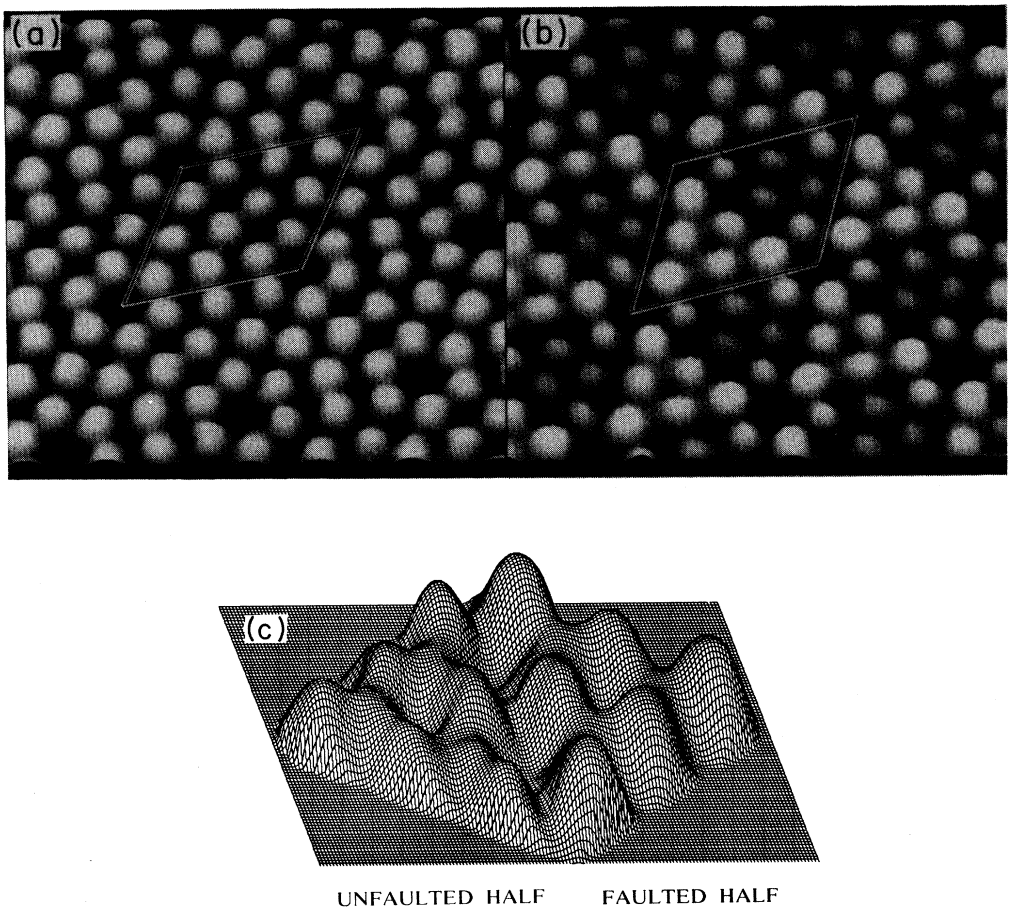

FIG. 2. STM topographs of the clean Si(111)-(7×7) surface. (a) Topograph of the unoccupied states obtained with the sample biased at +1.5 eV. The 7×7 unit cell is outlined and the 12 adatoms are clearly visible. (b) Topograph of the occupied states obtained with the sample biased at −1.5 V. The stacking fault and the differences between corner and center adatoms are visible. (c) A three-dimensional rendering of a topograph of the occupied states obtained with the sample biased at −3 V. The rest atoms are now visible.

surface. In Fig. 3, we show topographs of the unoccupied states of a partially reacted Si(111) surface. Topograph 3(a) is obtained after exposure to NH_3 ($\sim$2 L) under the same bias conditions. [1 langmuir (L)$\equiv 10^{-6}$ Torr sec.] We see that roughly half of all Si adatoms have become invisible (dark) as a result of the surface reaction. The surface appears as if it has been etched by the NH_3 reaction, while, as we discussed in the Introduction, the reaction is predominately one of dissociative chemisorption. If we increase the sample bias so as to image higher-lying unoccupied states we see that at +3 V [topograph 3(b)] we can image both reacted and unreacted adatoms. Interestingly, we find that the 7×7 reconstruction (dimer domain walls, corner holes, etc.) is preserved by the reaction with, as topograph 3(b) shows, some distortions. The behavior exhibited by the occupied states of the sample is even more interesting. As can be seen from Fig. 4(a), the topograph obtained with the sample biases at −2 V shows unreacted adatoms as bright spots, while reacted adatoms appear dark. This is completely analogous to the behavior of the unoccupied states. However, topograph 4(b) obtained at −3 V (i.e., by probing up to −3 eV below E_F) shows a significant change. Every site that appeared dark in Fig. 4(a) is now bright—in fact, it appears brighter than the unreacted sites of Fig. 4(a). To help locate corresponding sites at the two topographs we have labeled a few such sites. It is clear that at −3 V we can directly image the products of the surface reaction. Moreover, by inspecting topograph 4(b) we can see that it appears that there are two kinds of product sites distinguished by their "size." To help visualize this difference, we provide in Fig. 4(c) a three-dimensional view of sites $a-f$ shown, in Fig. 4(b). Sites a and c are reacted adatom sites. It appears that product site a is "larger" than site c. Because these topographs have been obtained in the constant-current mode, it is believed that size reflects the local density of states (LDOS) in the interval $E_F - eV_{\text{bias}}$. The above topographs suggest that there are two reaction products, or perhaps two different configurations of a product, whose spatial distribution can be directly determined by the STM. If what we image are two different products, it is of interest to establish

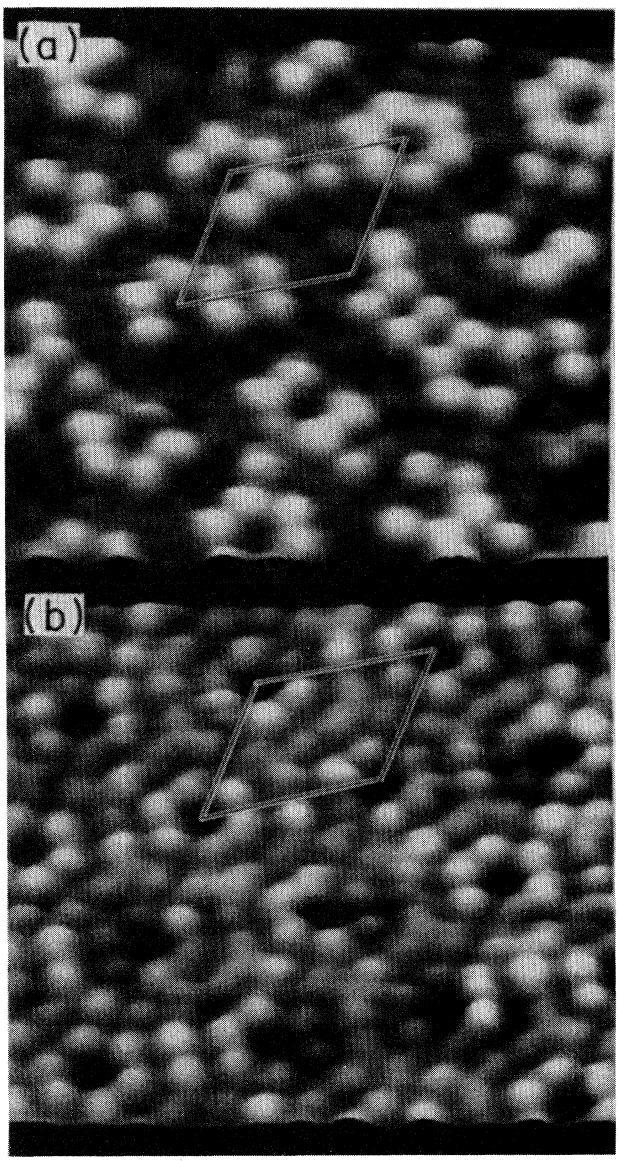

FIG. 3. (a) Topograph of the unoccupied states of a Si(111)-(7×7) surface partially reacted with NH_3. Sample bias +0.8 V. Reacted adatoms appear dark. (b) Topograph of the unoccupied states of a partially reacted surface. Sample bias +3 V. Both reacted and unreacted adatom sites are visible. The 7×7 reconstruction is preserved overall by the reaction.

their chemical identity. Using EELS (Ref. 10) and photoemission,[11,12] Si—H and Si—NH_2 groups have been identified as the reaction products. If indeed these are the two products that we image with the STM, then based on the relative contributions of these two species to the ultraviolet photoemission spectroscopy (UPS) spectra[11,12] (an experimental measure of LDOS) of the NH_3-exposed surface up to −3 eV, we would predict that the "larger" image represents the Si-NH_2 moiety, while the "smaller" one is a Si-H species. However, we should point out that there are still many unknown factors that make quantitative interpretation of STM images uncertain. In more than one case we have obtained topographs of the partially reacted surface at −3 V where the relative intensities of reacted and unreacted adatoms are reversed from those shown in Fig. 4. At these high biases, tip stability is a problem, due to primarily field-induced atomic rearrangements on the tip surface. In most cases, these tip changes only affect image resolution, but in some cases relative intensities are affected. The reason behind this behavior is not known but we speculate that this behavior may result because tunneling at the tip may involve chemically different atoms. The symmetry of the states involved in tunneling at the tip can thus be different, and some effective selection rules based on differences in wave-function overlap at different sites may become important. It is clear that such effects need to be further explored and understood for STM images to be quantitatively interpreted. One also can foresee that by controlling tip composition, the possibility of "chemically selective" imaging may be realized.

The above results clearly show that STM topographs obtained at different energies provide, for the first time, the unique capability of following both the extent and spatial distribution of a surface reaction on an atom-by-atom basis.

B. Atom-resolved tunneling spectra of clean and NH_3-exposed Si(111)-(7×7)

More detailed information about the electronic structure of the clean and reacted surface is provided by atom-resolved scanning tunneling spectroscopy (AR-STS). In addition, AR-STS provides a reliable way to probe the reactivity of the surface rest atoms. While, as Fig. 2(c) shows, rest atoms can be directly imaged, this imaging requires high-bias conditions, under which tip stability is often a problem. We found that AR-STS detection of rest atoms is relatively free from such complications. In Fig. 5(a) we show a topograph of the clean surface with a unit cell outlined, and underneath it we present AR-STS spectra obtained at the positions within the surface unit cell, indicated by the arrows. The spectra obtained at the representative surface sites, adatoms, and rest atoms are in complete agreement with area-integrated photoemission and inverse-photoemission spectra[14] and also with current-imaging results.[15] The spectrum obtained over a rest-atom site is given by curve A. It shows a strong surface state at $\sim$0.8 eV below the Fermi energy (E_F). Given this large binding energy with respect to E_F and the small value of the electron Coulomb repulsion, U, at that site ($\sim$0.4 eV),[16] we expect that the rest-atom dangling-bond state will be fully occupied by two electrons. The spectra obtained over the two adatom sites, corner adatoms (B) and center adatoms (C), are different. The signals from the occupied states (negative bias) are weak—in particular, those over center-adatom sites—while the reverse behavior is observed for the unoccupied states (positive sample bias). It has been argued that the quantity $(dI/dV)/(I/V)$ is (roughly) proportional to the local density of states (LDOS).[17] For sustained tunneling out of states in the gap, additional scattering processes must be involved to

maintain their electron population. Thus, the interpretation of the $(dI/dV)/(I/V)$ intensities of different surface states as providing a measure of their relative LDOS should be viewed with some caution if the states have significantly different energies. In the case of the adatoms, however, the energies of the corner- and center-adatom dangling-bond states are essentially identical. Thus, it is clear that the center-adatom site (C) has a lower occupied LDOS than the corner-adatom site (B). A simple interpretation of this difference, which is also in accord with theoretical prediction,[18] would be that there is transfer of charge from the adatom sites to the rest-atom site. Since there are two rest-atom neighbors for each center-adatom, while there is only one in the case of a corner adatom , a lower occupation is expected of the center-adatom DB state, in agreement with our observations here.

Next we consider the atom-resolved spectra of a partially reacted ($\sim 50\%$ of adatoms) surface [Fig. 5(b). With the tip over a rest-atom site we obtain spectrum A in Fig. 5(b). We note that the characteristic dangling-bond feature at -0.8 eV below E_F is absent, indicating that the rest-atom dangling bond has been saturated. The spectrum obtained over a reacted (dark) adatom site,

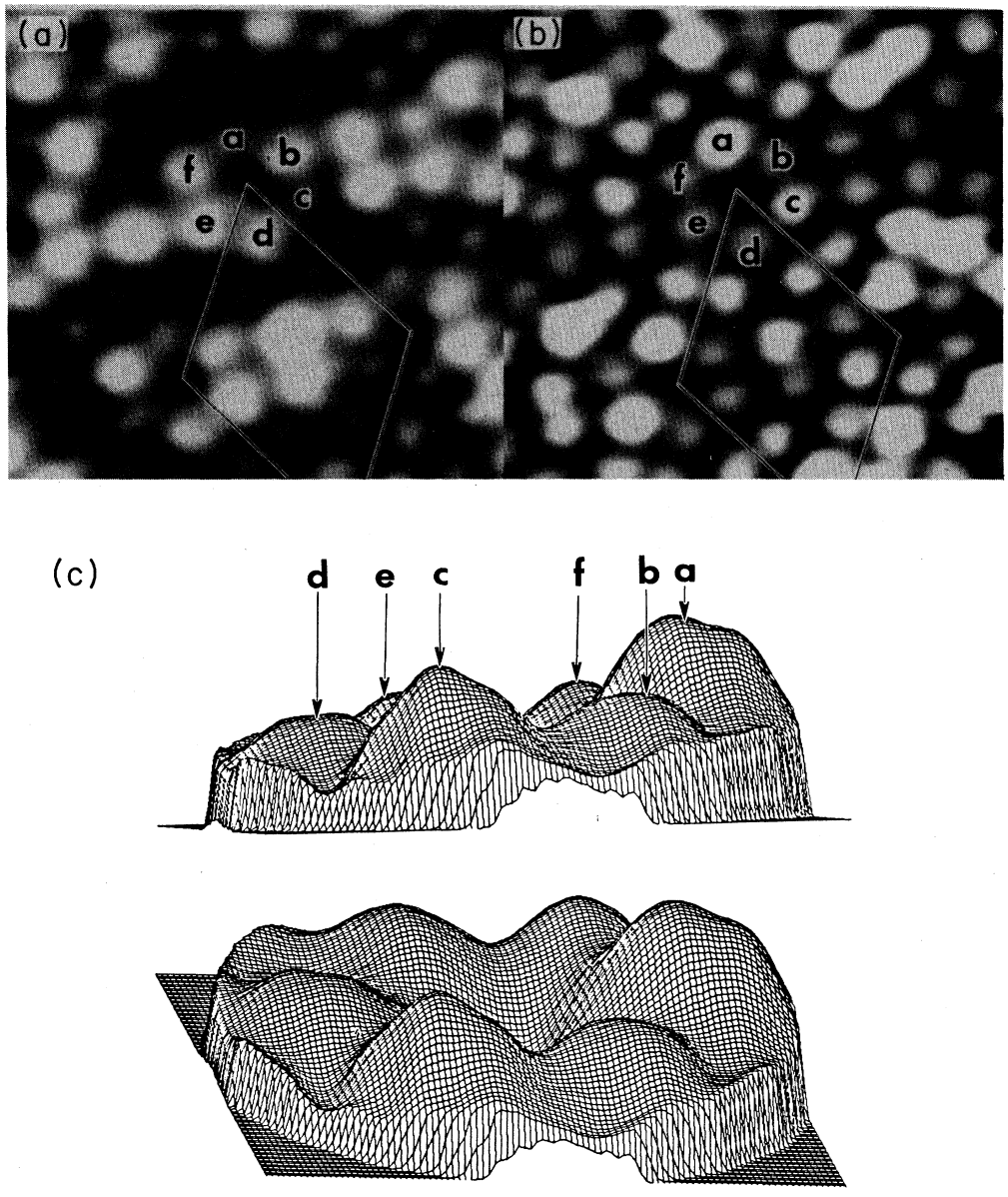

FIG. 4. (a) Topograph of the occupied states of the NH_3-exposed Si(111)-(7×7) surface (sample bias -2 V). Reacted adatoms appear dark. (b) Topograph obtained with the sample biased at -3 V. Reacted sites appear bright—compare corresponding sites in (a) and (b). (c) Three-dimensional topograph showing the labeled sites in (b). Sites b, d, e, and f are unreacted adatom sites, while a and c are reacted sites.

curve B (dashed line), shows that the characteristic low-energy adatom surface states have been eliminated. This observation explains why reacted adatoms appear dark for low sample biases. To access the relative reactivity of adatoms and rest atoms we have systematically analyzed large numbers of topographs and associated $(dI/dV)/(I/V)$ versus V spectral maps. Spectra are typically recorded at 1-Å intervals while simultaneously measuring a topograph. In this way, we find that rest atoms are more reactive than adatoms. Upon NH_3 exposure, rest atoms react first, and under conditions such as those of Fig. 5(b) where about half of the adatoms are still unreacted, we find no unreacted rest atoms remaining. On a surface such as that in Fig. 5(b), where the rest atoms have reacted, the spectra of *unreacted* adatoms become very interesting. As curves B—right (corner adatom) and C—right (center adatom) show, the spectra of the two adatom sites are now similar. Concentrating on spectrum C—right, and comparing it with the corresponding spectrum C—left, of the clean surface, we notice a reversal of the intensity distribution between occupied and unoccupied states. On the partially reacted surface the intensity of occupied states has increased, with a simultaneous decrease of the intensity of unoccupied states. To explain the low intensity of the center-adatom dangling-bond state at the clean surface, we proposed an adatom to rest-atom–charge-transfer process. This charge transfer will result in a nearly closed $(3s, 3p)$-shell

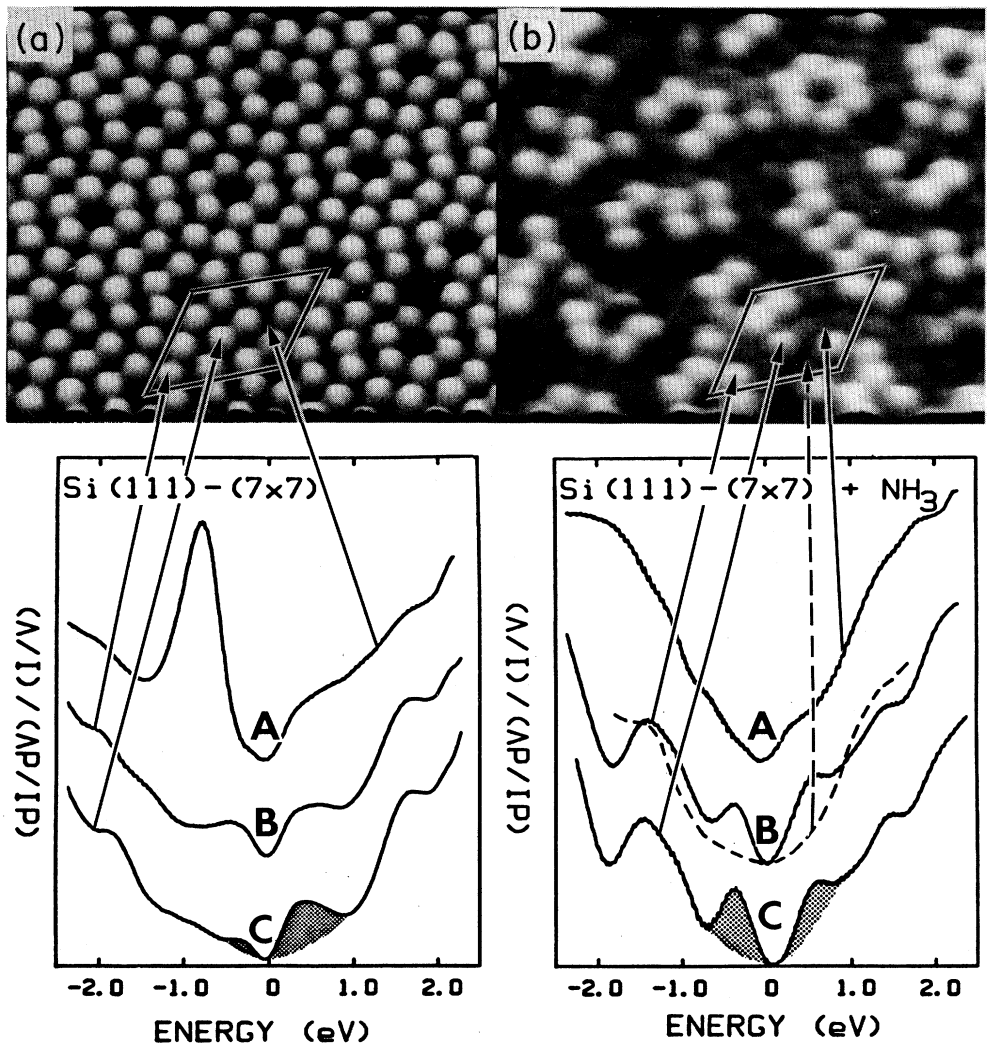

FIG. 5. (a) Topograph of the unoccupied states of the clean 7×7 surface (top) and atom-resolved tunneling spectra (below). Curve A gives the spectrum over a rest-atom site, curve B gives the spectrum over a corner-adatom site, and curve C gives the spectrum over a center-adatom site. Negative energies indicate occupied states, while positive energies indicate empty states. (b) Topograph of the unoccupied states (top) and atom-resolved tunneling spectra (below) of an NH_3-exposed surface. Curve A gives the spectrum over a *reacted* rest-atom site, curve B (dashed line) gives the spectrum over a *reacted* corner adatom, while curves B (solid line) and C give the spectra over *unreacted* corner and center adatoms, respectively.

rest atom. For a reaction to occur at that site, it may be energetically preferred to remove some of the excess charge; this can be achieved by a reverse charge transfer from rest atom to adatom. In addition to the changes induced to the dangling-bond states, we also see that the adatom backbond state at about -1.8 eV (Refs. 18 and 19) is removed, and in its place a new band at about -1.5 eV is observed. We tentatively suggest that this new band may be due to the adatom backbond state on the partially reacted surface. The adatom–rest-atom coupling must proceed via the backbonds. The rest-atom $\leftrightarrow$ adatom backbond interaction present at the clean surface will both broaden and increase the binding energy of the backbond state. Upon reaction, the rest-atom dangling-bond state is eliminated and is replaced by Si—X (X = H or NH_2) bonding and antibonding states far removed from E_F. As a result, the adatom backbond state will become uncoupled, its binding energy will then be decreased, and the reduction of the effective barrier will lead to an increased intensity.

C. The relative reactivity of surface dangling-bond states.

The preferential elimination of the rest-atom dangling-bond surface states upon exposure to NH_3 implies a higher chemisorption rate at these sites. This rate can be influenced by a variety of factors, including electronic effects which dictate the existence and magnitude of activation barriers, dissipative channels for the energy of incident reactants, steric constraints, surface diffusion, etc. Currently, there are no reactions at semiconductor surfaces for which the influence of all these factors is known. However, in the case of a reaction occurring at two sites of the same surface the situation may be somewhat simpler. Thus, in the case of the NH_3 reaction at adatom and rest-atom sites, factors such as energy dissipation are not expected to be significantly different. Diffusion of strongly bound species as H or NH_2 is not expected to take place and this is confirmed by experiment.[20] The 7×7 structure is quite open and we do not expect any strong differences in steric factors, which, if present, would probably favor reaction at adatom sites, contrary to our findings here. Thus, it is more likely that electronic factors control surface reactivity. This is in agreement with our previous finding that the reactivity of Si surfaces at low temperatures is determined by the dangling-bond surface states.[4,12] Referring to Fig. 6, we note that rest atoms represent normal triply coordinated Si sites. The adatoms, on the other hand, are located in threefold sites over a Si atom in the second layer. Each adatom participates in three four-member rings. This introduces strain in the backbonds and brings the adatom close to the Si atom directly below it (see Fig. 6). As a result of this bonding geometry, the three backbonds are weakened and give rise to the surface state at about 2 eV below E_F.[18,19] In addition, the proximity of the adatom to the

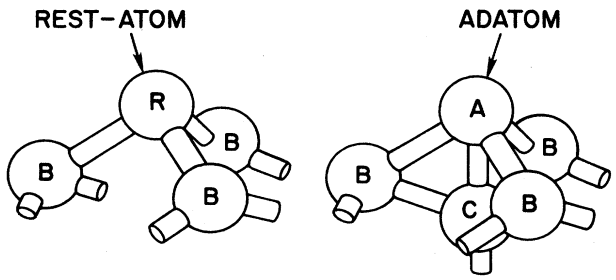

FIG. 6. The local structure of the rest-atom and adatom sites. Note the proximity and interaction between the adatom (A) and the Si atom (C) directly below it.

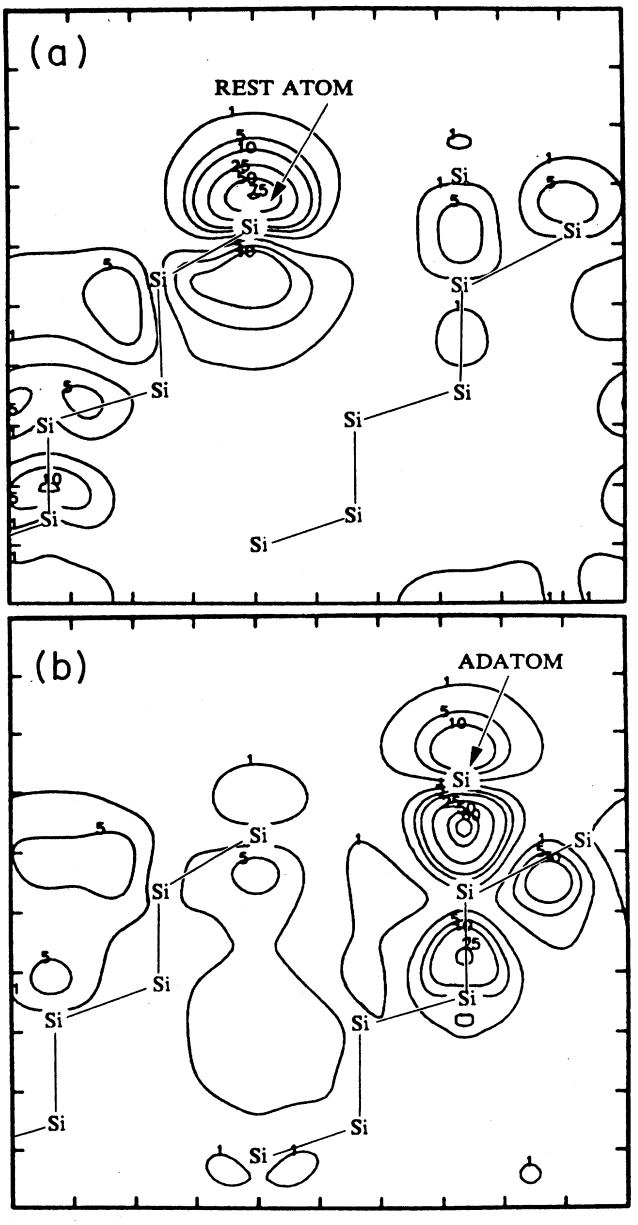

FIG. 7. Charge-density plots of (a) rest-atom and (b) adatom states near the Fermi energy. Note the concentration of charge in the region between the adatom and the Si atom directly below it (A—C bond in Fig. 6). From Ref. 21.

atom below it leads to the possibility of forming a weak fourth bond between the adatom and this subsurface atom. This bonding scheme is supported by recent first-principles electronic-structure calculations.[21] Because of the size of the 7×7 unit cell, a calculation for the actual unit cell will require immense computation. Instead, a model consisting of a 12-Si-atom-thick slab with a surface unit cell which includes one rest atom and one adatom was used. In Fig. 7 we show charge-density contours for the rest-atom dangling-bond state and the adatom "dangling-bond" state. The adatom state has its maximum DOS slightly above E_F so that it is only partially occupied, in agreement with spectra 5(B) and 5(C). While the contours at the rest-atom site are typical of a dangling-bond state, at the adatom site an accumulation of charge density between the adatom and the atom directly below it is observed, i.e., the formation of the fourth bond proposed above. The electron density on the vacuum side is reduced concomitantly. Experimental support for the existence of adatom–subsurface-Si-atom interactions was provided by a recent study of the vibrational spectra of the 7×7 surface.[22] In this study an unusually high vibrational frequency was observed and assigned as due to a local vibration involving the adatom and the Si atom underneath it. Consider now the reaction of rest atoms and adatoms, with an incoming species. At the rest-atom site, this process can be considered as a simple dangling-bond saturation process. However, at the adatom site the reaction will produce an essentially hypervalent (fivefold-coordinated) adatom. Silicon, unlike carbon, is known to form compounds in which it participates in five or even six bonds.[23] This hypervalency of Si is usually ascribed to the presence of the empty $3d$ levels and its larger size, which allows more bonds to be formed without overly increasing steric repulsion. Pentavalent Si compounds usually adopt a trigonal-bipyramid local structure.[23] Such a structure, however, would require that the three A-B backbonds [Fig. 6(b)] should be nearly coplanar, which clearly is not possible in this case. Thus, because of hypervalency and strain the bonding arrangement at adatom sites is less optimal for reaction than at rest-atom sites. Correspondingly, the activation barrier for reaction at adatom sites will be larger than that for reaction at rest-atom sites, leading to a faster reaction rate at the rest-atom sites, in agreement with our STM observations. The absolute magnitude of the activation energy at rest-atom sites should be quite small, as can be deduced from the fact that reaction occurs even at low temperatures.[12,24] We believe that this low activation energy is again a manifestation of the ability of Si to overcoordinate. Thus, unlike the case of carbon chemistry, a new bond can start forming without an old one being significantly weakened.

Because the arguments we used are general, we would expect that they also will be valid for other surface reactions. Indeed we find[24] that rest atoms are the preferred reaction sites in reactions involving several different closed-shell systems. We also find that these reactions tend to preserve the 7×7 reconstruction. Reactions of Si(111)-(7×7) with open-shell systems show more varied behavior in which adatom backbonds become active participants.[24]

Next, we consider the spatial distribution of the reaction within the adatom subset. In Fig. 8 we show a topograph of the unoccupied states of a 600×600 Å^2 area of the partially reacted surface. It is immediately clear that the majority of the unreacted adatoms appear in the six-member rings surrounding corner holes, i.e., they are corner adatoms. In fact, there can be more than four times more unreacted corner adatoms than unreacted center adatoms.

On the clean surface, we saw that the tunneling I-V measurements indicated differences between the corner- and center-adatoms dangling-bond states. It would be natural then to attribute the observed reactivity differences to the differences in electronic structure revealed by the studies on the clean surface. However, we found that rest atoms react before there is significant reaction among the adatoms. At a surface where the rest-atom dangling bonds have already been saturated, atom-resolved tunneling spectroscopy [Fig. 5(b)] shows that the electronic structure of the two adatoms sites becomes very similar. Another possibility for the observed reactivity difference could be that there is an interaction between rest-atom and adatom sites in the sense that reaction at a rest-atom site somehow directs one of the molecular fragments preferentially to center-adatom sites. If the fragments were statistically distributed to the adatom sites, it would lead at most to a 2:1 center-adatom to corner-adatom reactivity ratio, while experimentally this ratio is larger than 4:1. Moreover, our photoemission studies[24] show that at low temperatures (90 K) only the rest-atom surface state is quenched by NH_3 with no observable quenching of the adatom surface state. The same studies indicate that the reaction is the same at 300

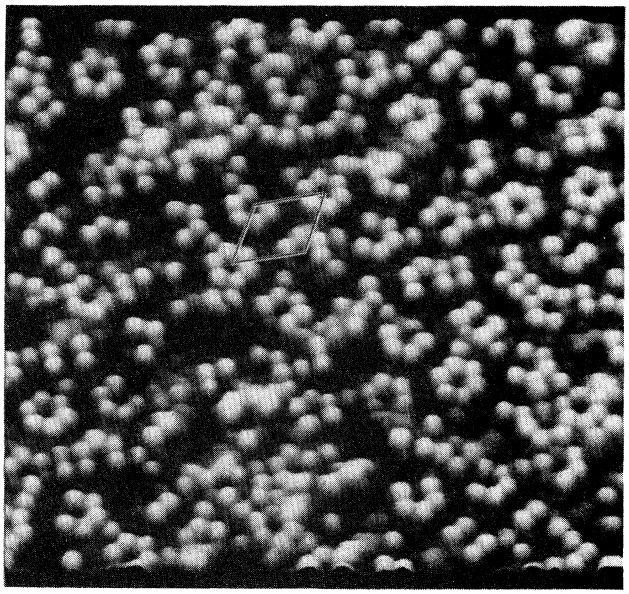

FIG. 8. STM topograph of the unoccupied states (sample bias +1 V) of a 600×600 Å^2 area of a partially reacted Si(111)-(7×7) surface. Note that the majority of the unreacted adatoms are adjacent to corner holes, i.e., they are corner adatoms.

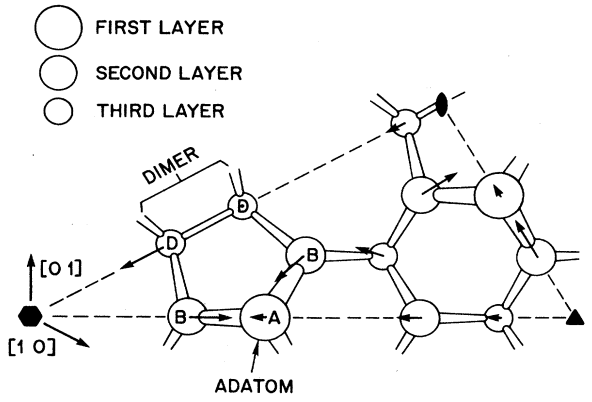

FIG. 9. Distortions of the ideal 7×7 structure determined by x-ray-diffraction experiments (Ref. 26). Arrows show the directions and relative size of the displacements from the starting ideal positions, exaggerated 10 times. Adapted from Ref. 26.

and 90 K. It appears, therefore, that the observed reactivity difference between the two adatom sites is due to intrinsic differences in the structure of these sites. Since the electronic structure of the dangling bonds is the same in the two sites [see Fig. 5(b)], we tentatively propose that the differences in reactivity involve backbonds; specifically, differences in strain energy of the corresponding late (i.e., productlike) transition states. Theoretical work[25] has suggested that the principal driving force for the 7×7 reconstruction is the formation of the dimer domain walls. X-ray-diffraction studies[26] find that the dimer bond is strained and its bond length is ~6% longer than the bulk Si—Si bondlength. As we discussed earlier, the adatoms also introduce distortions. The measured inward lateral contraction of the basal atoms (B) is rather large, ~0.1 Å.[26] The displacements determined in Ref. 26 are shown in Fig. 9. (For easier visualization, the displacements have been exaggerated by a factor of 10.) By reference to Fig. 9, we would expect that the contraction of A—B bonds would lead to the lengthening of the B—D bonds, which in turn allows the strengthening of the dimer bond (D—D). Upon saturation of the adatom dangling bonds the reverse sequence may be expected: the A—B bonds will be lengthened and the B—D bonds shortened, further straining the dimer bond. Inspection of the DAS 7×7 model (Fig. 1) shows that reaction at a corner adatom will strain two dimer bonds, while reaction at a center adatom will affect only one dimer bond. Qualitatively, the increased strain induced by reaction at a corner-adatom site would tend to increase the energy of the transition state, leading to a decreased reaction rate at that site.

IV. CONCLUSIONS

In conclusion, we have shown that by using topographs obtained at different energies, as well as atom-resolved electronic spectra, unreacted and reacted surface sites can be imaged selectively. Thus, surface electronic structure and reactivity can be studied on an atom-by-atom basis and the role of the local environment on the reactivity of surface dangling-bond sites can be evaluated. In the case of the reaction of Si(111)-(7×7) with NH_3, we find that rest-atom sites are more reactive than adatom sites. Moreover, center-adatom sites are more reactive than corner-adatom sites. We ascribe the reduced reactivity of adatoms to the delocalized nature of their dangling-bond state. Specifically, we suggest the formation of a weak bond between an adatom and the subsurface Si atom directly below it. Thus, while reaction at a rest-atom site can be considered as a simple dangling-bond saturation process, at an adatom site, reaction involves the formation of a hypervalent (fivefold-coordinated) adatom. At the clean surface, atom-resolved spectroscopy shows a lower occupation of the center-adatom dangling-bond state than that of the corner-adatom state. We ascribe this behavior to a more extensive adatom to rest-atom charge transfer at center-adatom sites. At a partially reacted surface, where the more reactive rest-atom dangling bonds have been saturated, we find that the tunneling spectra of unreacted corner and center adatoms become very similar. Thus, the reactivity differences found for the two adatom sites are not likely to be related to the initial occupation differences. We tentatively ascribe the observed reactivity differences to differences in adatom-induced strains of Si dimers. Atom-resolved spectroscopy provides the unique opportunity to probe directly the effect of chemisorption on the electronic structure and energy of *unreacted* surface sites. Thus, we find evidence for a reverse, i.e., rest atom to unreacted adatom, charge transfer upon rest-atom reaction.

ACKNOWLEDGMENTS

We would like to thank F. Bozso, K. Pandey, D. Vanderbilt, and E. Kaxiras for useful discussions, and R. Walkup for a careful reading of the manuscript.

[1]For reviews and collections of recent papers, see J. Vac. Sci. Technol. A **6**, 259 (1988); P. K. Hansma and J. Tersoff, J. Appl. Phys. **61**, R1 (1987); R. J. Behm and W. Hosler, in *Chemistry and Physics of Solid Surfaces VI,* edited by R. Vanselow and R. Howe (Springer-Verlag, Berlin, 1986).

[2]P. Hollins and J. Prichard, Prog. Surf. Sci. **19**, 275 (1985); R. F. Willis, A. A. Lucas, and G. D. Mahan, in *The Chemical Physics of Solid Surfaces and Heterogeneous Catalysis,* edited by D. A. King and D. P. Woodruff (Elsevier, Amsterdam, 1983), Vol. 2.

[3]M. A. Morris, M. Bowker, and D. A. King, in *Comprehensive Chemical Kinetics,* edited by C. H. Bamford, C. F. H. Tipper, and R. G. Compton (Elsevier, Amsterdam, 1984), Vol. 19.

[4]F. Bozso and Ph. Avouris, Phys. Rev. Lett. **57**, 1185 (1986); Ph. Avouris, F. Bozso, and R. Hamers, J. Vac. Sci. Technol. B **5**, 1387 (1987); R. J. Hamers, Ph. Avouris, and F. Bozso, Phys.

Rev. Lett. **59**, 2071 (1987).
[5]R. Wolkow and Ph. Avouris, Phys. Rev. Lett. **60**, 1049 (1988).
[6]R. E. Schlier and H. E. Farnsworth, *Semiconductor Surface Physics,* (Pennsylvania University Press, Philadelphia, 1957); J. Chem. Phys. **30**, 917 (1959).
[7]G. Binnig, H. Rohrer, C. Gerber, and E. Weibel, Phys. Rev. Lett. **50**, 120 (1983).
[8]K. Takayanagi, Y. Tanishiro, M. Takahashi, H. Motoyoshi, and K. Yagi, J. Vac. Sci. Technol. A **3**, 1502 (1985).
[9]M. Nishijima and K. Fujiwara, Solid State Commun. **24**, 101 (1977); T. Isu and K. Fujiwara, *ibid.* **42**, 477 (1982).
[10]S. Tanaka, M. Onchi, and M. Nishijima, Surf. Sci. **191**, L756 (1987).
[11]L. Kubler, E. K. Hlil, D. Bolmont, and G. Gewinner, Surf. Sci. **183**, 503 (1987).
[12]F. Bozso and Ph. Avouris, Phys. Rev. B **38**, 3943 (1988); Ph. Avouris, R. Wolkow, F. Bozso, and R. J. Hamers, Mater. Res. Soc. Symp. Proc. **105**, 35 (1988).
[13]At higher energies, R. S. Becker *et al.*, Phys. Rev. Lett. **55**, 2032 (1985), have found spectroscopic differences between the unoccupied states of the two halves of the 7×7 unit cell.
[14]F. J. Himpsel and Th. Fauster, J. Vac. Sci. Technol. A **2**, 815 (1984).
[15]R. J. Hamers, R. M. Tromp, and J. E. Demuth, Phys. Rev. Lett. **57**, 2979 (1986).
[16]J. E. Northrup (private communication).
[17]R. M. Feenstra, J. A. Stroscio, and A. P. Fein, Surf. Sci. **181**, 295 (1984).
[18]J. E. Northrup, Phys. Rev. Lett. **57**, 154 (1986).
[19]G-X. Qian and D. J. Chadi, J. Vac. Sci. Technol. A **5**, 906 (1987).
[20]B. G. Koehler, C. H. Mak, D. A. Arthur, P. A. Coon, and S. M. George, J. Chem. Phys. **89**, 1709 (1988).
[21]K. C. Pandey (unpublished).
[22]W. Daun, H. Ibach, and J. E. Muller, Phys. Rev. Lett. **59**, 1593 (1987).
[23]See, for example, N. N. Greenwood and A. Earnshaw, *Chemistry of the Elements* (Pergamon, Oxford, 1984).
[24]Ph. Avouris and F. Bozso (unpublished).
[25]D. Vanderbilt, Phys. Rev. Lett. **59**, 1456 (1987).
[26]I. K. Robinson, W. K. Waskiewicz, P. H. Fuoss, and L. J. Norton, Phys. Rev. B **37**, 4325 (1988).

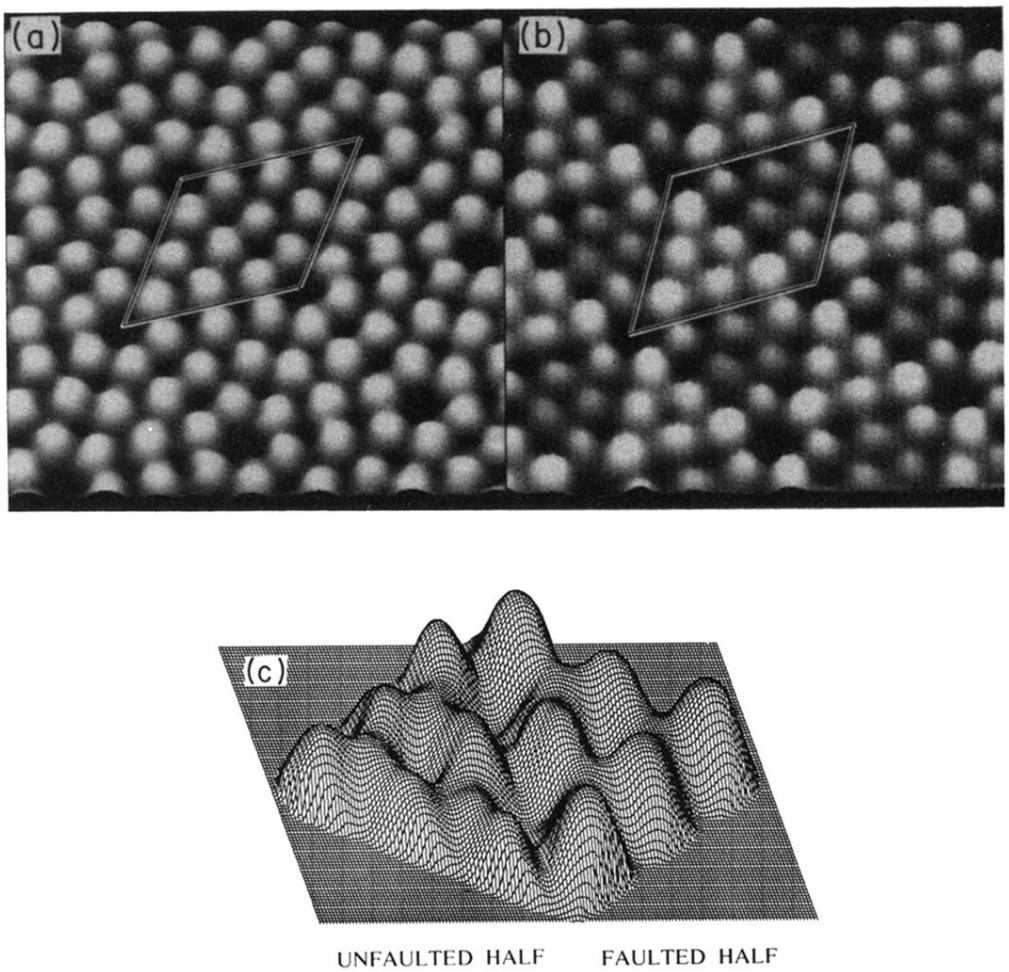

FIG. 2. STM topographs of the clean Si(111)-(7×7) surface. (a) Topograph of the unoccupied states obtained with the sample biased at +1.5 eV. The 7×7 unit cell is outlined and the 12 adatoms are clearly visible. (b) Topograph of the occupied states obtained with the sample biased at −1.5 V. The stacking fault and the differences between corner and center adatoms are visible. (c) A three-dimensional rendering of a topograph of the occupied states obtained with the sample biased at −3 V. The rest atoms are now visible.

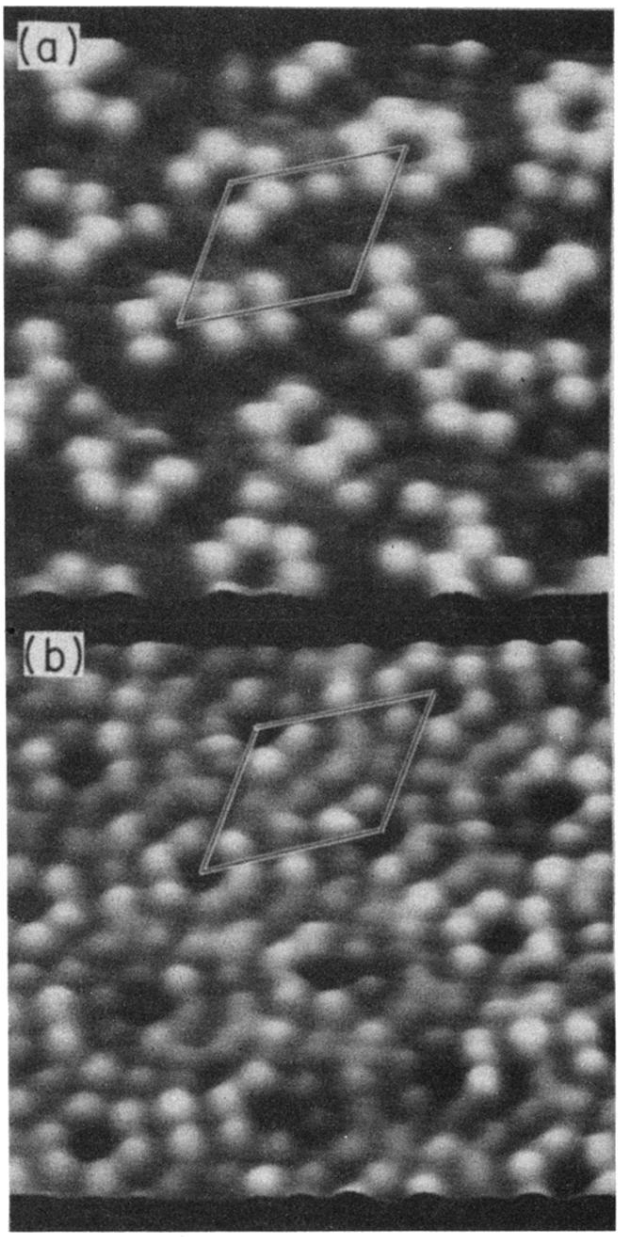

FIG. 3. (a) Topograph of the unoccupied states of a Si(111)-(7×7) surface partially reacted with NH_3. Sample bias +0.8 V. Reacted adatoms appear dark. (b) Topograph of the unoccupied states of a partially reacted surface. Sample bias +3 V. Both reacted and unreacted adatom sites are visible. The 7×7 reconstruction is preserved overall by the reaction.

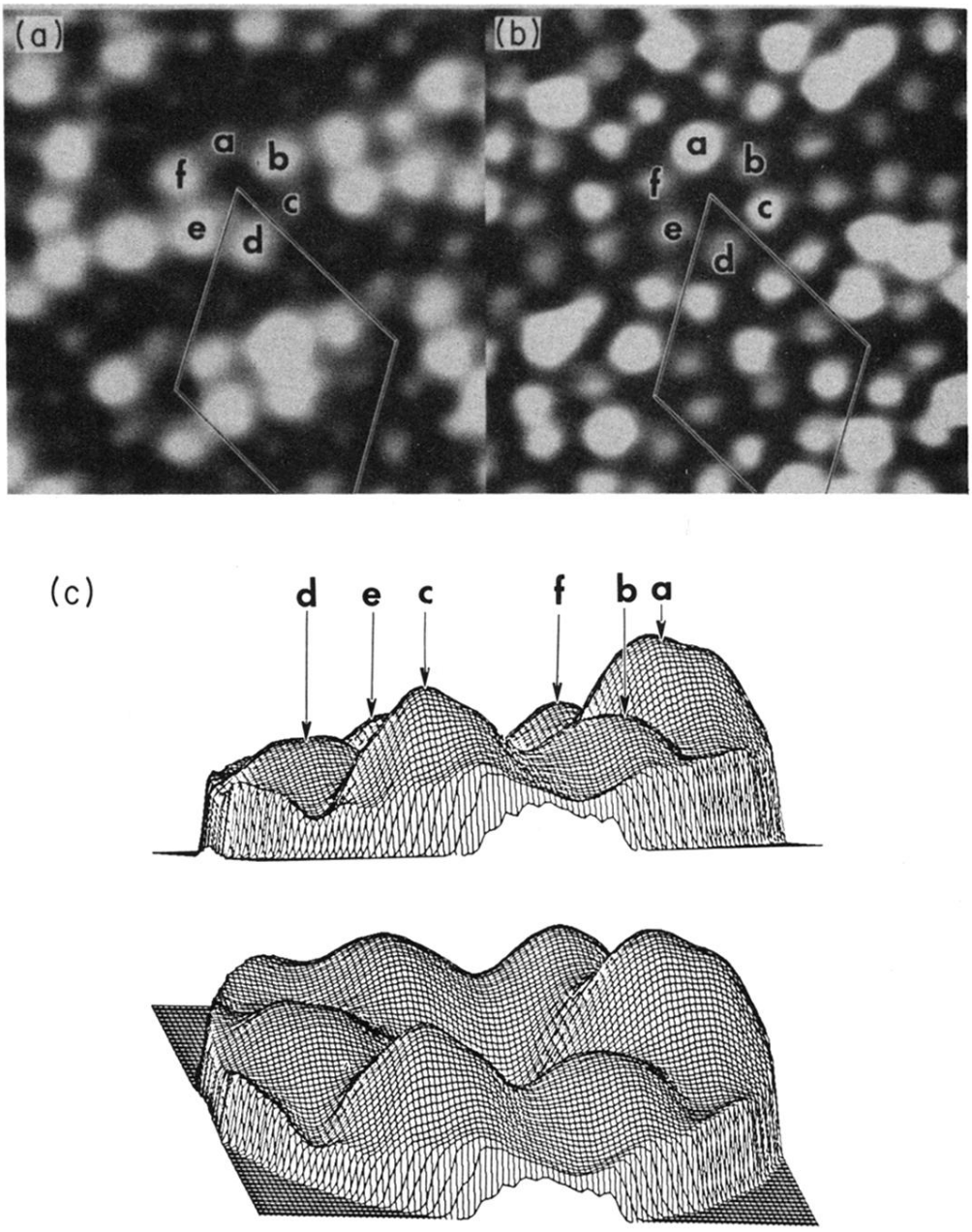

FIG. 4. (a) Topograph of the occupied states of the NH_3-exposed Si(111)-(7×7) surface (sample bias −2 V). Reacted adatoms appear dark. (b) Topograph obtained with the sample biased at −3 V. Reacted sites appear bright—compare corresponding sites in (a) and (b). (c) Three-dimensional topograph showing the labeled sites in (b). Sites *b*, *d*, *e*, and *f* are unreacted adatom sites, while *a* and *c* are reacted sites.

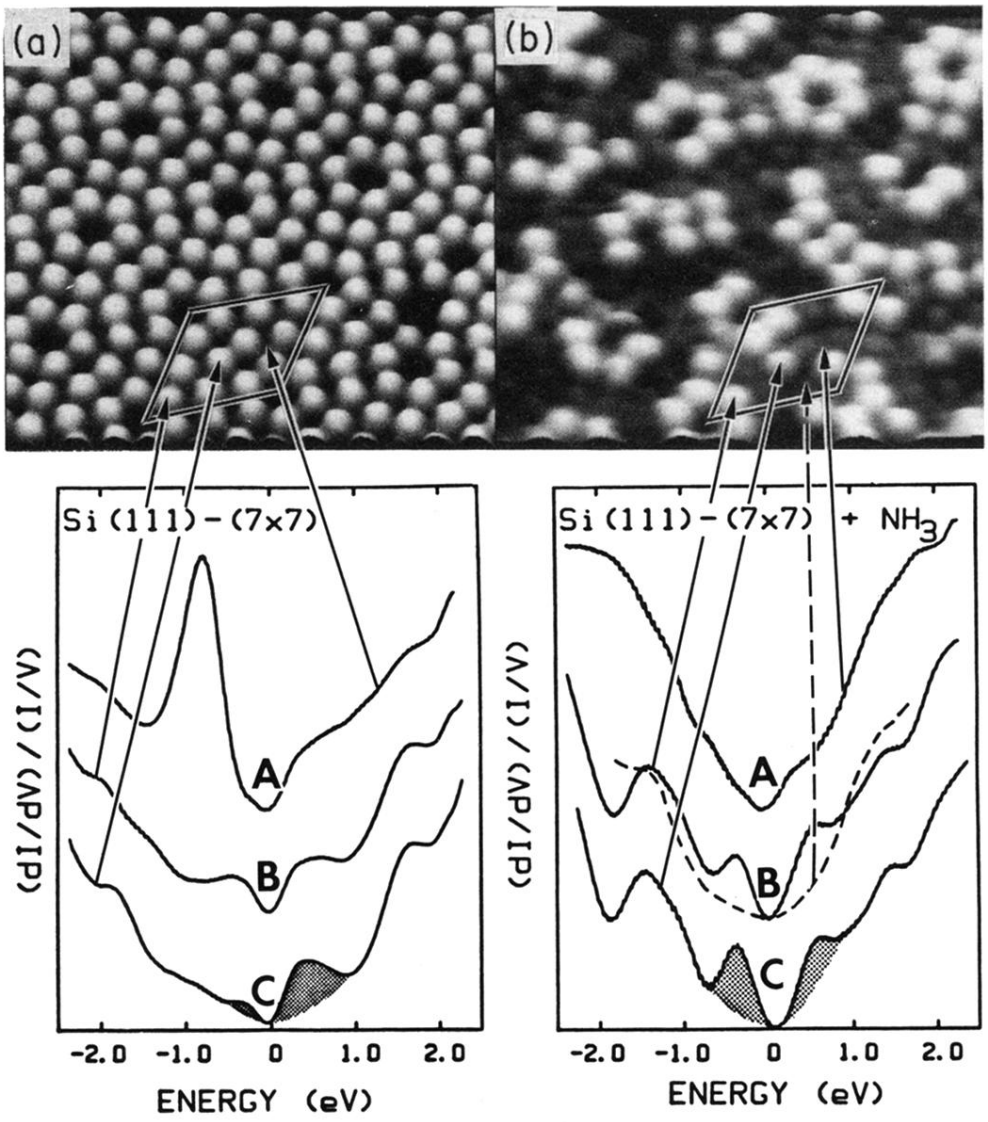

FIG. 5. (a) Topograph of the unoccupied states of the clean 7×7 surface (top) and atom-resolved tunneling spectra (below). Curve *A* gives the spectrum over a rest-atom site, curve *B* gives the spectrum over a corner-adatom site, and curve *C* gives the spectrum over a center-adatom site. Negative energies indicate occupied states, while positive energies indicate empty states. (b) Topograph of the unoccupied states (top) and atom-resolved tunneling spectra (below) of an NH_3-exposed surface. Curve *A* gives the spectrum over a *reacted* rest-atom site, curve *B* (dashed line) gives the spectrum over a *reacted* corner adatom, while curves *B* (solid line) and *C* give the spectra over *unreacted* corner and center adatoms, respectively.

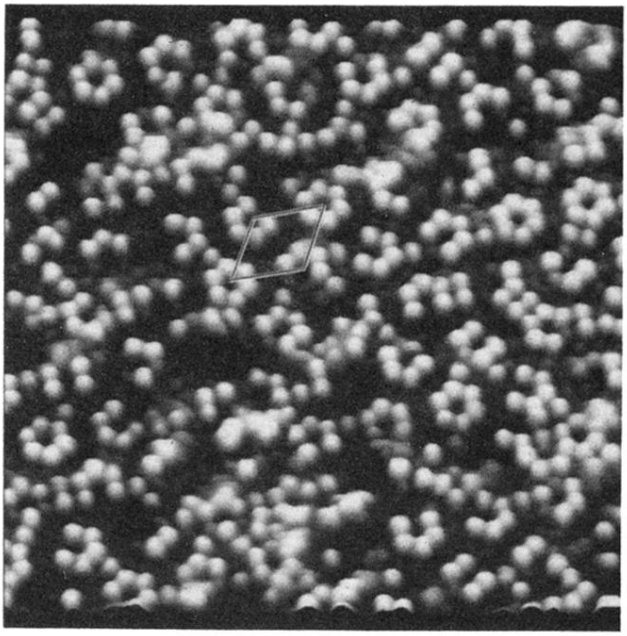

FIG. 8. STM topograph of the unoccupied states (sample bias +1 V) of a 600×600 Å^2 area of a partially reacted Si(111)-(7×7) surface. Note that the majority of the unreacted adatoms are adjacent to corner holes, i.e., they are corner adatoms.